



# Synthesis and characterization of Fe-containing biphasic calcium phosphate ceramics

Omer Kaygili<sup>1</sup>

Received: 14 February 2018 / Revised: 9 May 2018 / Accepted: 18 July 2018 / Published online: 2 August 2018  
© Australian Ceramic Society 2018

## Abstract

Three biphasic calcium phosphate (BCP) ceramics with various Fe contents (e.g., 0.66, 1.32, and 1.98 at.%) were prepared using wet chemical synthesis. X-ray diffraction (XRD), Fourier transform infrared (FTIR) spectroscopy, differential thermal analysis (DTA), thermogravimetric analysis (TG), scanning electron microscopy (SEM), and energy dispersive X-ray (EDX) spectroscopy techniques were used to characterize the as-prepared BCPs. The DTA and TG results show that the as-prepared samples are thermally stable. The addition of Fe affects significantly the lattice parameters, unit cell volume, and morphology. The EDX data confirm the introduction of Fe.

**Keywords** Hydroxyapatite · Wet chemical synthesis · Scanning electron microscopy (SEM) · X-ray diffraction (XRD)

## Introduction

Biphasic calcium phosphates (BCPs) are composed of hydroxyapatite (HAp,  $\text{Ca}_{10}(\text{PO}_4)_6(\text{OH})_2$ ) and beta-tricalcium phosphate ( $\beta$ -TCP,  $\text{Ca}_3(\text{PO}_4)_2$ ), which are members of calcium phosphate family [1–3]. Both HAp and  $\beta$ -TCP are biocompatible and osteoconductive materials that enable bone formation due to their compositions similar to the mineral phase of bone [4]. The molar ratios of Ca to P are 1.67 for HAp and 1.50 for  $\beta$ -TCP. HAp has a hexagonal crystal structure with the lattice parameters of  $a = b = 0.9418$  nm,  $c = 0.6884$  nm, and unit cell volume of  $V = 0.5288$  nm<sup>3</sup> [5]. The crystal structure of  $\beta$ -TCP is rhombohedral, but this phase is identified in the X-ray diffraction (XRD) analysis according to the Whitlockite phase with the trigonal structure [6]. Therefore, using the hexagonal setting, the lattice parameters and unit cell volume values belonging to the  $\beta$ -TCP phase are  $a = b = 1.0429$  nm,  $c = 3.7380$  nm, and  $V = 3.5208$  nm<sup>3</sup> (JCPDS pdf no: 09-0169). Both HAp and  $\beta$ -TCP have some prominent properties as-mentioned above for biomedical applications, but

neither HAp nor  $\beta$ -TCP is preferred alone in practice [7, 8]. BCPs have been extremely used in bone regeneration and tissue engineering applications due to their eminent properties such as biocompatibility, safety, good cell attachment, and similarity to mineral structure of bone tissue [9–11].

In the present study, the effects of Fe content on the crystal structure, thermal properties, and morphology of BCPs were investigated and reported in more detail.

## Materials and methods

### Synthesis

Biphasic calcium phosphate (BCP) samples with various Fe contents of 0.66, 1.32, and 1.98 at.% were synthesized via a wet chemical synthesis. The molar ratio of (Ca + Fe)/P was kept at the value of 1.50 for each sample. Diammonium hydrogen phosphate ( $(\text{NH}_4)_2\text{HPO}_4$ , Merck) was dissolved in the distilled water and the total amount of this solution was 100 ml. Calcium nitrate tetrahydrate ( $\text{Ca}(\text{NO}_3)_2 \cdot 4\text{H}_2\text{O}$ , Carlo Erba) and iron(III) nitrate nonahydrate ( $\text{Fe}(\text{NO}_3)_3 \cdot 9\text{H}_2\text{O}$ , Sigma–Aldrich) were also dissolved in the distilled water and 100 ml of solution was prepared. Then it was poured drop by drop into calcium nitrate solution. This mixture of 200 ml was continuously stirred in a magnetic stirrer

✉ Omer Kaygili  
okaygili@firat.edu.tr

<sup>1</sup> Department of Physics, Faculty of Science, Firat University, 23119 Elazig, Turkey

at 50 °C for 4 h. The as-prepared mixtures for each sample were completely dried by waiting in an oven at 185 °C for 15 h. The as-dried samples were calcined at 925 °C for 1 h and then biphasic calcium phosphate powders were obtained.

## Characterization

X-ray diffraction (XRD) analyses were carried out by a Rigaku RadB-DMAX II diffractometer using a CuK $\alpha$  radiation with wavelength of  $\lambda=0.15406$  nm produced at 40 kV and 40 mA, and the XRD data were recorded in the  $2\theta$  range from 20 to 60° at every 0.02° for the scan speed of 2° min<sup>-1</sup>. The Joint Committee on Powder Diffraction Standards (JCPDS) files were used to the matching and identifying the crystalline phases.

The functional groups in the as-synthesized samples were determined by a PerkinElmer Spectrum One Fourier transform infrared (FTIR) spectrometer in the wavenumber interval of 400–4000 cm<sup>-1</sup> using KBr pellets with a spectral resolution of 4 cm<sup>-1</sup>.

The morphological investigation and elemental analysis were performed on a scanning electron microscope operated at an accelerating voltage of 20 kV (SEM, LEO EVO 40xVP) equipped with an energy dispersive X-ray (EDX, Röntech xflash) spectrometer.

The thermal properties of the samples in the temperature range from 25 to 1000 °C at a heating rate of 10 °C min<sup>-1</sup> were investigated using the differential thermal analysis (Shimadzu DTA 50) and thermogravimetric analysis (Shimadzu TGA 50) experiments.

## Results and discussion

### XRD results

The XRD patterns of the as-synthesized BCPs depicted in Fig. 1 indicate that all the samples have the polycrystalline structure. Two phases of HAp (PDF no: 09–0432) with the hexagonal crystal system and  $\beta$ -TCP (PDF no: 09–0169) having the trigonal crystal system are detected for each sample, and this points out the formation of the BCP structure without observing an extra phase. While HAp is the major phase,  $\beta$ -TCP is the minor one for all the samples. As can be seen in Table 1, with increasing Fe content, the amount of HAp phase decreases, as a matter of course the amount of  $\beta$ -TCP increases.

For each sample, the crystallite size ( $D$ ) was calculated according to Scherrer equation using the crystal planes of (0 0 2) and (0 2 10) for HAp and  $\beta$ -TCP phases, respectively [12]:

$$D = \frac{0.9\lambda}{\beta \cos \theta} \quad (1)$$

where  $\beta$  is the full width at half maximum (FWHM) and  $\theta$  is the diffraction angle. The calculated values of the  $D$  for each phase in the samples are given in Table 1. It is seen that the crystallite size value belonging to each phase gradually decreases with increasing amount of Fe. This gradual decrease in the crystallite size means that Fe ions replace with Ca ions in the BCP structure since the ionic radius of Fe (0.0645 nm) is smaller than that of Ca (0.099 nm) [13].

**Fig. 1** XRD patterns of the as-synthesized Fe-containing BCPs

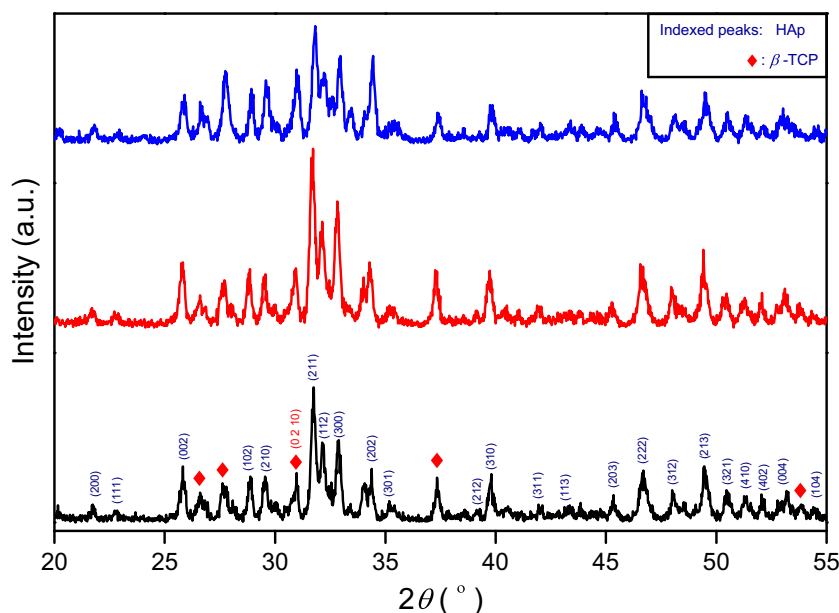


**Table 1** The calculated values of the crystallite size, crystallinity percent, phase composition, lattice parameters, and unit cell volume for each sample

Sample	Phase composition (%)		$X_C$ %	HAp				$\beta$ -TCP			
	HAp	$\beta$ -TCP		$D_{002}$ (nm)	$a$ (nm)	$c$ (nm)	$V$ (nm <sup>3</sup> )	$D_{0210}$ (nm)	$a$ (nm)	$c$ (nm)	$V$ (nm <sup>3</sup> )
FT1	74.9	25.1	92.82	29.98	0.9445	0.6901	0.5331	28.72	1.0507	3.7293	3.5654
FT2	73.4	26.6	91.47	28.92	0.9434	0.6896	0.5315	28.34	1.0466	3.7471	3.5545
FT3	61.8	38.2	90.41	28.04	0.9406	0.6875	0.5267	28.15	1.0458	3.7254	3.5285

Using the total area under crystal peaks ( $\sum A_C$ ) and total area under amorphous peaks ( $\sum A_A$ ) values, the crystallinity degree ( $X_C\%$ ) for each sample was computed using the following relation [14]:

$$X_C\% = \frac{\sum A_C}{\sum A_C + \sum A_A} \times 100 \tag{2}$$

The crystallinity degree decreases dramatically with increasing amount of Fe. As can be seen in Table 1, the weight percent of the  $\beta$ -TCP phase increases with Fe content. A gradual decrease in the crystallinity degree can be related to the increasing amount of the  $\beta$ -TCP phase [15]. The lattice parameters ( $a$  and  $c$ ) were computed for both HAp and  $\beta$ -TCP phases using the hexagonal setting [12]:

$$\frac{1}{d^2} = \frac{4}{3} \left( \frac{h^2 + hk + k^2}{a^2} \right) + \frac{l^2}{c^2} \tag{3}$$

where  $d$  is the distance for two adjacent planes, and  $h$ ,  $k$ , and  $l$  are the Miller indices. The volume of the hexagonal unit cell was calculated by the following relation [12]:

$$V = 0.866a^2c \tag{4}$$

For both phases, the descending values of the  $a$ ,  $c$ , and  $V$  with increasing Fe content are seen from Table 1. As mentioned before, the decrease in these parameters points out that Ca ions are replaced by Fe ions with the smaller ionic radius in comparison to Ca.

**FTIR results**

The FTIR spectra of the as-synthesized BCPs are shown in Fig. 2. The bands known as the characteristic vibrational modes of the hydroxyl group are detected at 3572 and 630  $\text{cm}^{-1}$  [16, 17]. The bands related to the vibrational modes of the phosphate group are observed at 1087, 1046, 1026, 962, 875, 599, and 562  $\text{cm}^{-1}$  [18, 19]. The band at 1407  $\text{cm}^{-1}$  is due to the vibrational modes of the carbonate group [20]. A gradual decrease, supporting the decrease in the crystallinity degree obtained from the XRD results, in the sharpness of the

bands of 1026, 599, and 562  $\text{cm}^{-1}$ , is observed with increasing amount of the dopant of Fe.

**SEM observations and EDX analysis**

The SEM images and EDX analysis of the as-prepared BCPs are given in Fig. 3. The morphological differences are observed. It could be possible to say that the particle size decreases with increasing Fe content, supporting the XRD results. The EDX reports indicate that there is no impurity in the samples, and these confirm the introduction of Fe into the BCP structure, as well as the increase in Fe content. The molar ratio of Ca/P is calculated to be 1.81, 1.72, and 1.64 for FT1, FT2, and FT3, respectively, indicating the Ca deficiency. The (Ca + Fe)/P molar ratio is calculated as 1.85, 1.82, and 1.80 for FT1, FT2, and FT3, respectively. Both molar ratios decrease with increasing amount of Fe.

**Thermal analysis of the BCPs**

The DTA curves of the samples are plotted in Fig. 4, and these curves imply that all the samples are thermally stable from 25 to 1000  $^\circ\text{C}$  since neither an endothermic nor an exothermic peak is observed. Figure 5 shows the TG curves of the as-synthesized BCPs. For all the samples, there is almost no significant change in the mass percent in the temperature range from 25 to

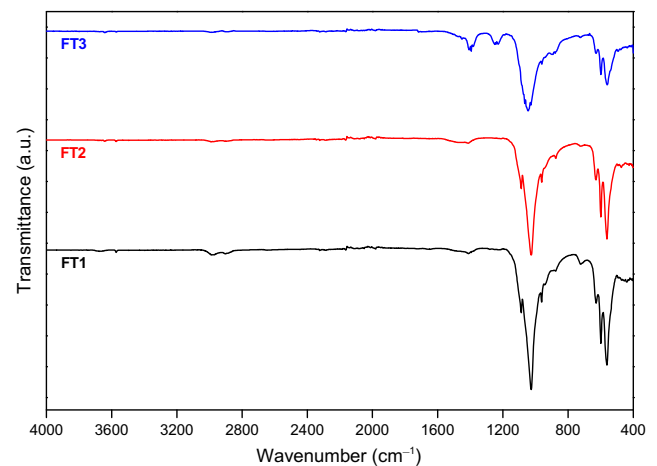


**Fig. 2** FTIR spectra for the as-prepared BCP samples doped with Fe

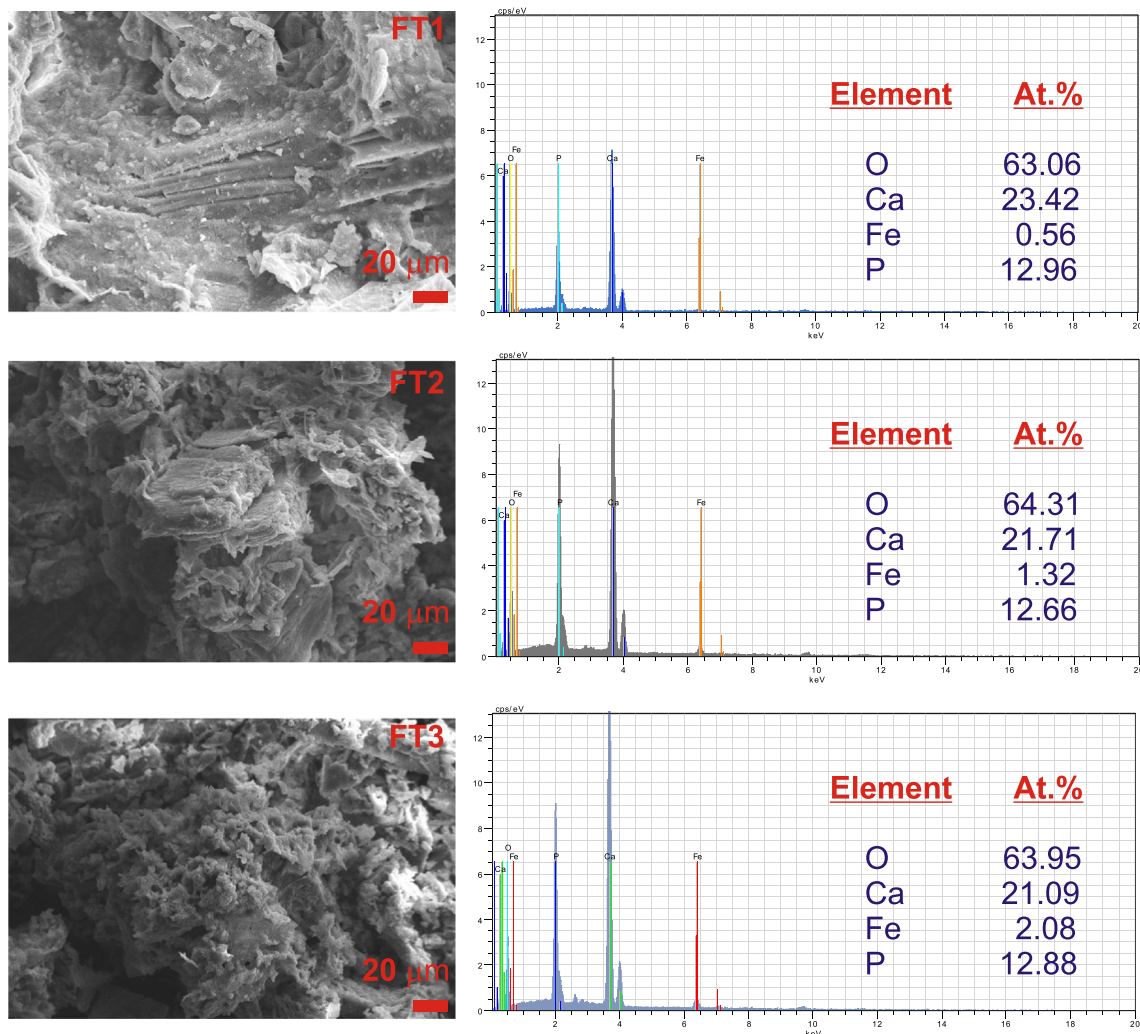


**Fig. 3** SEM images and EDX analysis results of the BCPs

1000 °C. In this temperature interval, an increase in the mass percent was observed for all the samples. These increases are found to be 0.95, 1.68, and 2.39%, for

FT1, FT2, and FT3, respectively. The thermal analysis curves, shown in Figs. 4 and 5, are in perfect harmony with the results reported by Raynaud et al. [21].

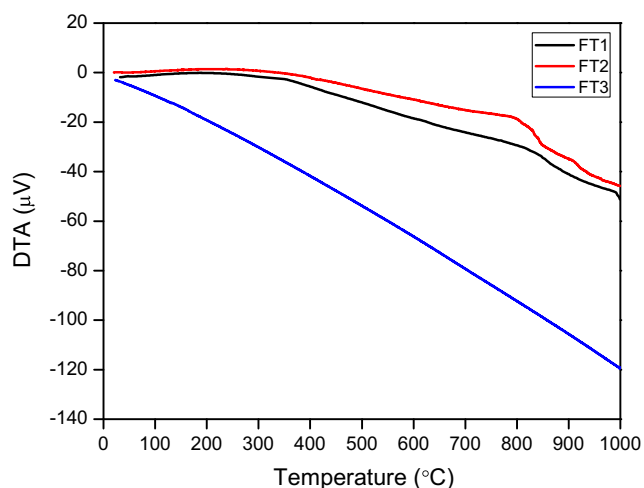


**Fig. 4** DTA curves of the samples

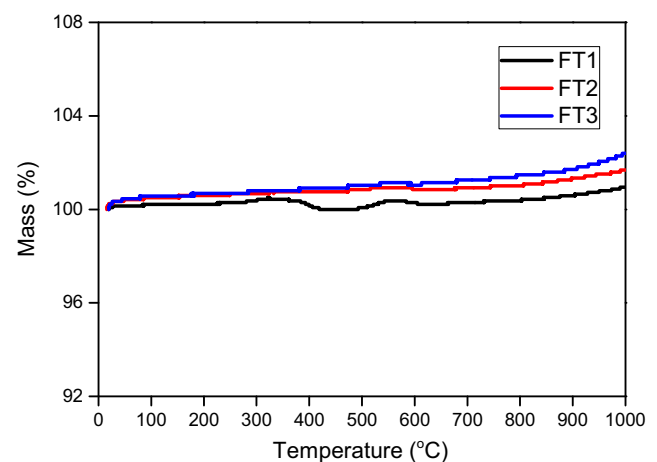


**Fig. 5** TG curves of the as-prepared BCP samples

## Conclusions

If the findings are evaluated as a whole, it is possible to arrive at the following conclusions. BCP ceramics with various Fe contents of 0.66, 1.32, and 1.98 at.% can be easily synthesized using the wet chemical method. In the temperature interval of 25–1000 °C, all the samples are thermally stable and there is no any excessive mass change. The introduction of Fe and no impurity are detected for each sample. The lattice parameters ( $a$  and  $c$ ), unit cell volume, crystallite size, crystallinity degree, and amount of HAp phase decrease gradually with the addition of Fe. In other words, all the as-mentioned parameters can be controlled by Fe content.

## References

- Legeros, R.Z., Lin, S., Rohanizadeh, R., Mijares, D., Legeros, J.P.: Biphasic calcium phosphate bioceramics: preparation, properties and applications. *J. Mater. Sci. Mater. Med.* **14**, 201–209 (2003)
- Dorozhkin, S.V.: Calcium orthophosphates (CaPO<sub>4</sub>): occurrence and properties. *Prog. Biomater.* **5**, 9–70 (2016)
- Kaygili, O., Keser, S.: Sol–gel synthesis and characterization of Sr/Mg,Mg/Zn and Sr/Zn co-doped hydroxyapatites. *Mater. Lett.* **141**, 161–164 (2015)
- Dorozhkin, S.V.: Calcium orthophosphates: applications in Nature, Biology, and Medicine. Pan Stanford, Singapore (2012)
- Liou, S.C., Chen, S.Y., Lee, H.Y., Bow, J.S.: Structural characterization of nano-sized calcium deficient apatite powders. *Biomaterials.* **25**, 189–196 (2004)
- Ernich, M., Peters, F.: X-ray powder diffraction data of synthetic  $\beta$ -tricalcium phosphate. *Mater. Werkst.* **37**, 526–529 (2006)
- Natasha, A.N., Singh, R., Abd Shukor, M.H.B., Young, T.C., Purbolaksono, J., Sopyan, I., Toulouei, R.: Synthesis and properties of biphasic calcium phosphate prepared by different methods. *Adv. Mater. Res.* **970**, 20–25 (2014)
- Albayrak, O.: Structural and mechanical characterization of boron doped biphasic calcium phosphate produced by wet chemical method and subsequent thermal treatment. *Mater. Charact.* **113**, 82–89 (2016)
- Lobo, S.E., Arinze, T.L.: Biphasic calcium phosphate ceramics for bone regeneration and tissue engineering applications. *Materials (Basel)*. **3**, 815–826 (2010)
- Ebrahimi, M., Botelho, M.G., Dorozhkin, S.V.: Biphasic calcium phosphates bioceramics (HA/TCP): concept, physicochemical properties and the impact of standardization of study protocols in biomaterials research. *Mater. Sci. Eng. C.* **71**, 1293–1312 (2017)
- Bouler, J.M., Pilet, P., Gauthier, O., Verron, E.: Biphasic calcium phosphate ceramics for bone reconstruction: a review of biological response. *Acta Biomater.* **53**, 1–12 (2017)
- Cullity, B.D.: Elements of X–ray Diffraction. 2nd Ed. Addison–Wesley Publishing Company, Massachusetts (1978)
- Kanchana, P., Lavanya, N., Sekar, C.: Development of amperometric L-tyrosine sensor based Fe-doped hydroxyapatite nanoparticles. *Mater. Sci. Eng. C.* **35**, 85–91 (2014)
- Kaygili, O., Tatar, C.: The investigation of some physical properties and microstructure of Zn-doped hydroxyapatite bioceramics prepared by sol–gel method. *J. Sol-Gel Sci. Technol.* **61**, 296–309 (2012)
- Kaygili, O., Dorozhkin, S.V., Ates, T., Al-Ghamdi, A.A., Yakuphanoglu, F.: Dielectric properties of Fe doped hydroxyapatite prepared by sol-gel method. *Ceram. Int.* **40**, 9395–9402 (2014)
- Mohammadi, Z., Mesgar, A.S.M., Rasouli-Disfani, F.: Preparation and characterization of single phase, biphasic and triphasic calcium phosphate whisker-like fibers by homogenous precipitation using urea. *Ceram. Int.* **42**, 6955–6961 (2016)
- Garai, S., Sinha, A.: Three dimensional biphasic calcium phosphate nanocomposites for load bearing bioactive bone grafts. *Mater. Sci. Eng. C.* **59**, 375–383 (2016)
- Abutalib, M.M., Yahia, I.S.: Novel and facile microwave-assisted synthesis of Mo-doped hydroxyapatite nanorods: characterization, gamma absorption coefficient, and bioactivity. *Mater. Sci. Eng. C.* **78**, 1093–1100 (2017)
- Yahia, I.S., Shkir, M., Alfaify, S., Ganesh, V., Kilany, M.: Facile microwave-assisted synthesis of Te-doped hydroxyapatite nanorods and nanosheets and their characterizations for bone cement applications. *Mater. Sci. Eng. C.* **72**, 472–480 (2017)
- Zarkesh, I., Ghanian, M.H., Azami, M., Bagheri, F., Baharvand, H., Mohammadi, J., Eslaminejad, M.B.: Facile synthesis of biphasic calcium phosphate microspheres with engineered surface topography for controlled delivery of drugs and proteins. *Colloids Surf. B: Biointerfaces.* **157**, 223–232 (2017)
- Raynaud, S., Champion, E., Bernache-Assollant, D., Thomas, P.: Calcium phosphate apatites with variable Ca/P atomic ratio I. Synthesis, characterisation and thermal stability of powders. *Biomaterials.* **23**, 1065–1072 (2002)